



Influence of ciliated protozoa and heterotrophic nanoflagellates on the fate of primary production in NE Atlantic Ocean.

Hera Karayanni, Urania Christaki, France van Wambeke, Michel Denis,
Thierry Moutin

► To cite this version:

Hera Karayanni, Urania Christaki, France van Wambeke, Michel Denis, Thierry Moutin. Influence of ciliated protozoa and heterotrophic nanoflagellates on the fate of primary production in NE Atlantic Ocean. . Journal of Geophysical Research. Oceans, 2005, 110 (C07S15), pp.7 - 15. 10.1029/2004JC002602 . hal-01780276

HAL Id: hal-01780276

<https://hal.science/hal-01780276>

Submitted on 4 Jul 2018

HAL is a multi-disciplinary open access archive for the deposit and dissemination of scientific research documents, whether they are published or not. The documents may come from teaching and research institutions in France or abroad, or from public or private research centers.

L'archive ouverte pluridisciplinaire **HAL**, est destinée au dépôt et à la diffusion de documents scientifiques de niveau recherche, publiés ou non, émanant des établissements d'enseignement et de recherche français ou étrangers, des laboratoires publics ou privés.

Influence of ciliated protozoa and heterotrophic nanoflagellates on the fate of primary production in the northeast Atlantic Ocean

Hera Karayanni,^{1,2} Urania Christaki,^{2,3} France Van Wambeke,¹ Michel Denis,¹ and Thierry Moutin⁴

Received 16 July 2004; revised 16 September 2004; accepted 23 November 2004; published 15 June 2005.

[1] Heterotrophic nanoflagellates and ciliates and their herbivorous activity were studied within the framework of the Programme Océan Multidisciplinaire Méso Echelle (POMME) in the northeastern Atlantic between 16°–22°W and 38°–45°N during winter, spring, and late summer/autumn 2001. Ciliate ingestion rates of *Synechococcus* and eukaryotic algae were measured using fluorescently labeled prey. Heterotrophic nanoflagellate ingestion rates of *Synechococcus* and *Prochlorococcus* were also estimated. Heterotrophic nanoflagellate and ciliate standing stock within the surface layer (0–100 m) showed seasonal variation, with maximal values in spring (866 mg C m⁻² and 637 mg C m⁻², respectively). Oligotrichs dominated the ciliate assemblages, except at one site visited during spring, where a tintinnid bloom was observed. Ingestion of photosynthetic cells less than 10 µm in size was positively correlated ($r = 0.7$, $p < 0.05$, $n = 12$) with primary production and accounted for 2–94% of this. Phytoplankton consumption reflected differences in the evolution of the phytoplankton bloom and in the structure of the microbial food web, both associated with the strong mesoscale hydrodynamic variability of the study area. In that context it is worthy to note that when tintinnids reached high abundances locally (1260 cells L⁻¹), their impact as phytoplankton grazers was important and reached 69% of primary production. Generally, heterotrophic nanoflagellates and ciliates were relatively more important in determining the fate of phytogenic carbon during spring. Another interesting feature of primary production consumption was that during the autumn, when *Prochlorococcus* dominated the phytoplankton community, the protozoan grazing activity was ineffective in regulating the fate of primary producers.

Citation: Karayanni, H., U. Christaki, F. Van Wambeke, M. Denis, and T. Moutin (2005), Influence of ciliated protozoa and heterotrophic nanoflagellates on the fate of primary production in the northeast Atlantic Ocean, *J. Geophys. Res.*, 110, C07S15, doi:10.1029/2004JC002602.

1. Introduction

[2] Protozooplankton is a ubiquitous and abundant component of the microzooplankton community in a large number of aquatic systems. This group is mainly represented by heterotrophic nanoflagellates and ciliates which are generally the major grazers in oceanic systems where pico- and nanoplankton dominate biomass and primary production [Kuipers and Witte, 2000; Sanders *et al.*, 2000; Burkill *et al.*, 1995]. In addition, the planktonic food web structure influences the fate of primary production in

the ocean and has consequences for the CO₂ transfer process. It is generally understood that when small phytoplankton cells or bacteria dominate the microbial community, the grazers of picoplankton are small protozoa which do not produce rapidly sinking faecal pellets. Several grazing steps are necessary to allow primary production to be incorporated into the upper trophic levels. Therefore most of the carbon fixed by phytoplankton is respired and remineralized by the microbial community in the surface mixed layer and there is little or no net uptake of CO₂ from the atmosphere to the sea. In contrast, when large phytoplankton cells dominate, they can either be deposited to the bottom [Maar *et al.*, 2002] or be grazed by copepods and other mesozooplankton which do produce rapidly sinking faecal pellets [Fortier *et al.*, 1994].

[3] Thus it is particularly important to get knowledge on fate of primary production in the North Atlantic as it is a major site of CO₂ flux. In that area remote sensing data show that the phytoplankton bloom is one of largest biological signals on the planet [Lewis, 1989]. The impact of microzooplankton on the primary production has been investigated in several previous studies in the northeast

¹Laboratoire de Microbiologie, Géochimie et Ecologie Marines, CNRS/INSU, UMR 6117, Centre d'Océanologie de Marseille, Université de la Méditerranée, Campus de Luminy, Marseille, France.

²Hellenic Centre for Marine Research, Anavissos, Greece.

³Now at Université du Littoral Côte d'Opale, CNRS-INSU, UMR 8013, Wimereux, France.

⁴Laboratoire d'Océanographie et de Biogéochimie, CNRS/INSU, UMR 6535, Centre d'Océanologie de Marseille, Université de la Méditerranée, Campus de Luminy, Marseille, France.

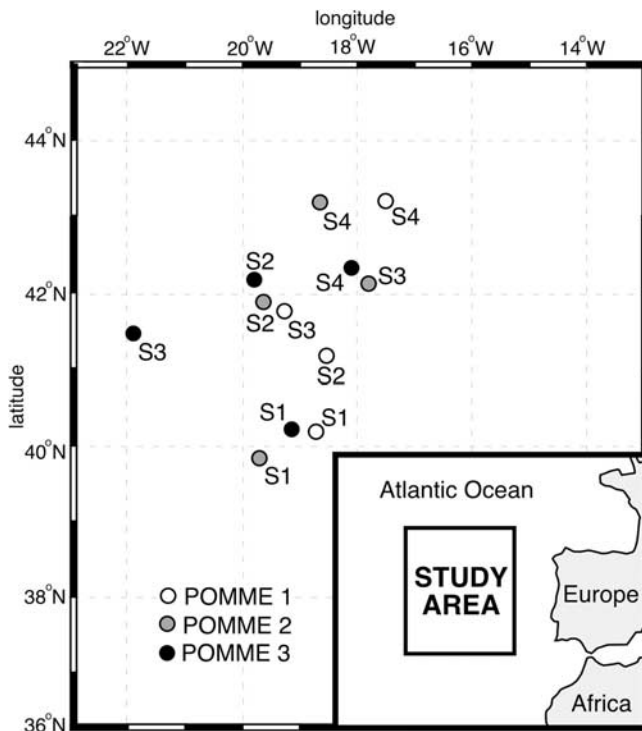


Figure 1. Study area and approximate location of sampling sites of the present study (P1, winter cruise; P2, spring cruise; P3, late summer–autumn cruise).

Atlantic, conducted within the frameworks of different national and international projects, for example NABE (1989), MLML (1991) PRIME (1996) and CANIGO (1998). Using community approaches (dilution method [Landry and Hassett, 1982]), these studies have shown that microzooplankton may consume more than 100% of the primary production in the subtropical and temperate northeast Atlantic during the spring and summer [Burkill et al., 1993; Verity et al., 1993; Weeks et al., 1993; Gifford et al., 1995; Stelfox-Widdicombe et al., 2000; Quevedo and Anadón, 2001]. Large heterotrophic flagellates and/or naked ciliates dominated the microzooplankton north of 47°N [Burkill et al., 1993; Verity et al., 1993; Gifford et al., 1995] while a transition to a heterotrophic community dominated by smaller cells (<20 μm) was observed in the studies conducted in the southern oligotrophic provinces where picoplankton dominated [Stelfox-Widdicombe et al., 2000; Quevedo and Anadón, 2001]. The dilution method employed in these studies, however, does not permit the measurement of the grazing impact of individual consumers. Their importance in carbon flux can be only hypothesized

according to their relative contribution to the abundance or biomass of the microzooplankton assemblage. In addition, these previous studies focused on the southern oligotrophic waters or the temperate northern waters under spring or summer conditions [Burkill et al., 1993; Verity et al., 1993; Gifford et al., 1995; Stelfox-Widdicombe et al., 2000; Quevedo and Anadón, 2001]. The present mesoscale study was centered in the intermediate zone between the northern and southern northeast Atlantic (16°–22°W, 38°–45°N) known as one of the zones of formation and subduction of modal waters [Paillet and Arhan, 1996]. Moreover, in an effort to provide a continuum of food web structure and function, sampling was performed on a seasonal scale (winter, spring, autumn). The evolution of the community structure of photosynthetic (<10 μm) and protozoan (ciliates and heterotrophic nanoflagellates) communities was studied, while the impact of individual predator groups on primary production was estimated by the method of fluorescently labeled prey [Sherr et al., 1987; Rublee and Gallegos, 1989] and a linear regression model [Christaki et al., 2002].

2. Materials and Methods

2.1. Study Site

[4] Sampling was conducted in the northeast Atlantic Ocean within the framework of the Programme Océan Multidisciplinaire Méso Echelle (POMME). The study covered an area of 375000 km² centered on 41.5°N, 19°W (500 km east-west by 750 km north-south; 16°–22°W/38°–45°N) (Figure 1). Measurements were made at four stations located in different hydrological structures (eddies, fronts, Table 1) during winter (February–March, POMME 1 (P1)), spring (April–May, POMME 2 (P2)), and autumn (September–October, POMME 3 (P3)) 2001. Three hydrological structures, one cyclonic (C4) and two anticyclonic eddies (A1 in the north and A2 in the south) were identified and sampled during the different seasons (Table 1).

2.2. Sampling and Counting of Ciliated Protozoa and Heterotrophic Nanoflagellates

[5] Sampling was always conducted at midday. For ciliate enumeration, 200–250 mL samples were taken from the upper 100 m at different depths (5, 10, 20, 30, 40, 50, 60, 80, 100 m). Each sample was gently mixed and then decanted into an opaque glass bottle and fixed with borax-buffered formaldehyde (2% final concentration). The samples were then stored at 4°C in the dark until analysis. In the laboratory, samples were left to settle for 3–4 days at 4°C. The bottom 100 mL of the sample was transferred into Hydrobios settling chambers, allowing it to settle for a minimum of 16 hours and then examined with an Olympus

Table 1. Sampling Sites and Dates and Related Hydrological Structures During the Three Programme Océan Multidisciplinaire Méso Echelle (POMME) Cruises (P1, P2, and P3)^a

	S1	S2	S3	S4
P1	A2 (1 March), 18.7°W–40.1°N	FR (6 March), 18.6°W–41.1°N	C4 (10 March), 19.2°W–41.8°N	A1 (14 March), 17.4°W–43.3°N
P2	A2 (17 March), 19.8°W–39.8°N	C4 (22 April), 19.7°W–41.9°N	SP (26 April), 17.7°W–42.1°N	A1 (1 May), 18.8°W–43.3°N
P3	A31 (19 Sept.), 19.1°W–40.1°N	C4 ^b (23 Sept.), 19.8°–42.2°N	C4 (27 Sept.), 22.0°W–41.5°N	C31 ^b (2 Oct.), 18.0°W–42.4°N

^aAbbreviations are as follows: A, anticyclonic eddy; C, cyclonic eddy; FR, front; SP, saddle point.

^bSites located on the boundary of corresponding eddy.

Table 2. Biovolumes and Average Diameters (\pm SD) of Heterotrophic Nanoflagellates (HN) and Photosynthetic Nanoeukaryotes (nEUK) During Winter (P1), Spring (P2), and Autumn (P3) Cruises^a

	HN		nEUK	
	μm^3	μm	μm^3	μm
P1	8.5	2.5 ± 0.3	25.8	3.7 ± 0.4
P2	14.6	3.0 ± 0.3	17.9	3.2 ± 0.4
P3	5.7	2.2 ± 0.2	15.9	3.1 ± 0.3

^aBiovolumes are in μm^3 and diameters are in μm .

IX-70 inverted microscope equipped for transmitted light, phase contrast and epifluorescence microscopy (at $400\times$). Blue light excitation (DM 500 nm dichroic mirror, BP 450 to 480 nm exciter filter, BA 515 nm barrier filter and a 100 W mercury burner) was used to detect chlorophyll autofluorescence and to distinguish plastidic from nonplastidic ciliates. Loss of cells due to fixation with formalin was compensated by applying a correction factor derived by counts in Lugol's solution. For this reason, a large data set ($n = 110$) representing multiple sampling depths from different hydrological structures visited during the study was analyzed as described by Karayanni *et al.* [2004]. Ciliates in each sample were enumerated and assigned to either aloricate ciliates or tintinnids. The former comprised taxa of Oligotrichida and Choreotrichida and the latter loricate species (order Choreotrichida, suborder Tintinnina [Montagnes and Lynn, 1991]). Aloricate ciliates were grouped into four taxa on the basis of shape, size, visible ciliature and morphology, and identified wherever possible to the species level based on Maeda and Carey [1985] and Maeda [1986]. Tintinnids were identified based on the lorica shape and dimensions by reference to Jørgensen [1924] and Kofoid and Campbell [1929]. Empty loricas were counted separately [Karayanni *et al.*, 2004]. Standard geometric shapes and conversion factors $190 \text{ fgC } \mu\text{m}^{-3}$ [Putt and Stoecker, 1989] were considered in order to calculate biomass of all taxa present in the samples [Karayanni *et al.*, 2004]. For tintinnid biovolumes, linear dimensions of the lorica were measured and 30% cell occupancy was considered [Gilron and Lynn, 1989]. However, small tintinnids (lorica volume $< 9 \times 10^3 \mu\text{m}^3$) appeared to occupy a greater percentage of the lorica volume and a 50% cell occupancy was assumed [Beers and Stewart, 1967; Tsuda *et al.*, 1989].

[6] To enumerate heterotrophic nanoflagellates (HN), 20–30 mL samples were preserved with ice cold glutaraldehyde at a final concentration of 1%. Samples were kept at 4°C in the dark, filtered on black Nuclepore filters (pore size $0.6 \mu\text{m}$) and stained with DAPI [Porter and Feig, 1980] within a few hours of sampling and stored at -20°C until counting. HN were enumerated using an Olympus AX-70 PROVIS epifluorescence microscope at $1000\times$. Autofluorescence (chlorophyll) was determined under blue light excitation (as for plastidic ciliates). To quantify the biomass of HN, linear dimensions of 30–50 cells from 40 m depth at each station visited (a total of 350–370 cells per cruise) were measured using an ocular micrometer. Furthermore, we compared the equivalent spherical diameters measured at different sampling sites during each season (P1, P2, and P3) using a one-way ANOVA. In all three cases, the

ANOVA test did not show any statistically significant difference ($p > 0.05$) between linear dimensions of HN. Consequently, an average equivalent spherical diameter for each cruise was considered in order to calculate biovolumes (Table 2). Biovolumes were converted to biomass using $220 \text{ fgC } \mu\text{m}^{-3}$ [Børsheim and Bratbak, 1987]. Abundance and biomass standing stocks were calculated by the integration of sampling depths between 0 and 100 m.

2.3. Sampling and Counting of Pico- and Nanophytoplankton

[7] For photosynthetic cell counts (*Synechococcus*, *Prochlorococcus*, picoeucaryotes and nanophytoplankton) 5 mL samples were prefiltered ($100 \mu\text{m}$ mesh size), preserved with 2% paraformaldehyde [Troussellier *et al.*, 1995] and stored in liquid nitrogen until laboratory analysis. Counts were obtained using a Cyturon Absolute (Ortho Diagnostic Systems) flow cytometer equipped with a laser exciting at 488 nm. Each cell was characterized by five optical parameters: two diffraction parameters (forward and right angle scatter) and three fluorescence parameters related to emissions in the red ($> 620 \text{ nm}$), orange (565–592 nm) and green (515–530 nm) wavelength ranges. Just before analysis, samples were rapidly thawed in a 30°C water bath. In order to calibrate the flow cytometer and to provide a reference for the concentration calculation, fluorescent beads, 1–10 μm in diameter, with green fluorescence emission were added to the samples. Data were collected and stored in list mode with the Immunocount II software (Ortho Diagnostic Systems) and cluster analyses were performed with the Winlist software (Verity Software House, Inc.). *Synechococcus* and *Prochlorococcus* cell numbers were converted to carbon biomass by applying conversion factors of $250 \text{ fgC cell}^{-1}$ [Kana and Glibert, 1987] and 49 fgC cell^{-1} [Cailliau *et al.*, 1996] respectively. To quantify the biomass of picoeucaryotes and nanophytoplankton (PN) cell biovolumes were calculated and converted to biomass using $220 \text{ fgC } \mu\text{m}^{-3}$ [Børsheim and Bratbak, 1987]. In order to calculate picoeucaryote biovolume, an average diameter of $1.8 \mu\text{m}$ and a scheme of a sphere were considered. PN linear dimensions were measured by epifluorescence microscopy and biovolumes were calculated as described for HN (25.8, 17.9, and $15.9 \mu\text{m}^3$ for P1, P2, and P3, respectively). Abundance and biomass standing stocks were calculated as for heterotrophs.

2.3.1. Preparation of Fluorescently Labeled Prey

[8] Two types of fluorescently labeled prey were made from cultures of *Synechococcus* WH8103 (FLS: Fluorescently Labeled *Synechococcus*) $\sim 1.0 \mu\text{m}$ in diameter, and *Nannochloropsis* sp. (FLA: Fluorescently Labelled Algae), 3–4 μm in diameter, to act as analogues of *Synechococcus* and photosynthetic eukaryotic cells $< 10 \mu\text{m}$ in diameter, respectively. *Synechococcus* WH 8103 was provided by the Roscoff Biological Station, France and *Nannochloropsis* sp. by SELONDA Aquaculture Enterprise, Greece. Cultures were grown in 250 mL sterile flasks in PCR-S11 medium in aged seawater, at $18 \pm 0.5^\circ\text{C}$ under continuous light ($15 \mu\text{mol quanta m}^{-2} \text{ s}^{-1}$), provided by cool white fluorescent bulbs wrapped in moonlight blue filters (Lee filter, Panavision France). Concentrations in the early stationary cultures used for the preparation of FLS and FLA were 10^8 and $10^7 \text{ cells mL}^{-1}$ respectively.

[9] Fluorescently labeled *Synechococcus* and algae were prepared according to Rublee and Gallegos [1989] adapted from Sherr *et al.* [1987]. Cells were harvested by centrifugation at $9500 \times g$ for *Synechococcus* and $2400 \times g$ for *Nannochloropsis* sp., resuspended in phosphate buffer and incubated at 60°C with 5-(4,6-dichlorotriazin-2-yl) amino-fluorescein (DTAF) (0.2 mg mL^{-1}). DTAF-stained cells were stored in 1 mL aliquots at -20°C . FLA were stored in 10% dimethyl-sulfoxide (DMSO) to minimize cell damage due to freezing in the phosphate buffer [Sherr *et al.*, 1991].

2.3.2. Grazing Experiments

[10] Grazing experiments were conducted at two depths within the euphotic zone, near surface (5 m) and close to the in situ fluorescence maximum (40–60 m), at all sampling stations occupied during each cruise. Water samples (1.2 L) were collected in duplicate into polycarbonate bottles, previously soaked in 10% HCl and rinsed with Milli-Q water, and remained untreated in the dark for 30–60 min at in situ temperature, to allow grazers to recover from handling. One prey analogue (FLS or FLA) was added to each duplicate sample in concentrations corresponding to 10^4 mL^{-1} to 10^2 – 10^3 mL^{-1} for FLS and FLA, respectively. After the addition of the prey analogs, subsamples were immediately taken for T_0 counts of FLS and FLA. Subsamples for ciliate vacuole content analysis (250 mL) were taken at 0, 15, 30 min and fixed immediately with 2% borated formalin. Samples were stored in opaque glass bottles and stored in the dark at 4°C until analysis. In the laboratory, ciliate abundance and FLA and FLS vacuole content were enumerated using inverted microscopy, in phase contrast and epifluorescence mode at $400\times$. Uptake rates of fluorescently labeled prey (FLS or FLA ciliate $^{-1} \text{ h}^{-1}$) were calculated for 15 min incubation times in most experiments as after 30 min the average number of FLS or FLA per ciliate had leveled off. Ingestion rates of *Synechococcus* sp. and photosynthetic picoeukaryotes and nanoplankton (cells CIL $^{-1} \text{ h}^{-1}$) were then calculated by multiplying the ingestion rate of FLP (Fluorescently Labeled Prey) by the ratio of abundances of natural prey to added FLP [Sherr *et al.*, 1987; Pace *et al.*, 1990]. Comparison of uptake rates measured at the surface and the fluorescence maximum depths did not show any statistically significant differences (paired t -test, $p > 0.05$) and consequently an average ingestion rate of the two measurements was calculated. Total carbon consumption ($\text{mg C m}^{-2} \text{ d}^{-1}$) for the whole water column was obtained by the integration over the upper 100 m.

2.3.3. Estimation of Grazing of *Synechococcus* and *Prochlorococcus* by HN

[11] Ingestion rates of *Prochlorococcus* and *Synechococcus* by HN were calculated using a linear regression model derived from a recent experimental study dealing with nanoflagellate predation on *Synechococcus* and *Prochlorococcus* [Christaki *et al.*, 2002]. In that study, ingestion rates (IR) of *Synechococcus* were found to increase for concentrations from 10^3 to 10^5 Syn mL^{-1} according to the linear regression equation

$$\text{IR}_{\text{Syn}} = -0.00130 + 0.0035 \times [\text{SYN mL}^{-1}], \quad r^2 = 0.903, \quad p < 0.001. \quad (1)$$

While ingestion rates on *Prochlorococcus* were found to increase for concentrations from 10^3 to $10^6 \text{ Proc mL}^{-1}$ according to the linear regression equation

$$\text{IR}_{\text{Proc}} = 0.0115 + 0.0012 \times [\text{PROC mL}^{-1}], \quad r^2 = 0.922, \quad p < 0.001. \quad (2)$$

All results presented below correspond to the sampling depths where grazing experiments of ciliates were conducted (5 m and fluorescence maximum).

2.3.4. Primary Production

[12] Carbon absorption was quantified using the ^{14}C method according to the experimental protocol detailed by Moutin and Raimbault [2002]. Samples (320 mL polycarbonate bottle, three light and one dark sample per depth, 7 to 8 depths) were collected before sunrise using 12 L Niskin bottles, inoculated with $20 \mu\text{Ci}$ of $\text{NaH}^{14}\text{CO}_3$ (Amersham CFA3) just before sunrise, and then incubated in situ. After 24 hours, the samples were filtered on $2 \mu\text{m}$ polycarbonate filters deposited on GF/F filters to measure net absorption ($A_N \text{ mgC m}^{-3}$) above and under $2 \mu\text{m}$ filter size. Filters were then covered with $500 \mu\text{L}$ of HCl 0.5 M and stored for counting at the laboratory. Each day three samples were filtered immediately after inoculation for t_0 determination, and $250 \mu\text{L}$ of sample was taken at random from three bottles and stored with $250 \mu\text{L}$ of ethanolamine to determine the quantity of added tracer (Q_i). In the laboratory, samples were dried over 12 hours at 60°C , the 10 mL of ULTIMA-GOLD-MV (Packard) were added to the filters and dpm was counted after 24 hours with a Packard Tri carb 2100 TR liquid scintillation analyzer.

[13] Daily (24 hours dawn to dawn) primary production (PP) was obtained from the difference between light and dark bottles measurements. Integrated primary production IPP ($\text{mg m}^{-2} \text{ d}^{-1}$) was calculated assuming that (1) subsurface (about 5 m) rates are identical to surface rates (not measured) and that (2) rates are zero at 20 m below the deepest sampled depth (below the photic zone).

3. Results

3.1. Hydrological Features

[14] Mean temperature at 5 m was about 14°C in winter (P1) and varied slightly in spring (P2) while higher values were recorded during autumn (P3) when mean temperature was about 21°C . However, the mixed layer depth varied strongly between sampling sites reflecting the particularities of each sampling site and latitudinal variations [Maixandau *et al.*, 2005]. The euphotic zone was relatively constant during P1 and P2 (40–60 m) and was over 80 m during P3 [Maixandau *et al.*, 2005].

3.2. Abundance and Biomass of Ciliated Protozoa and Heterotrophic Nanoflagellates

[15] During the three sampling periods variations of both ciliates and heterotrophic nanoflagellate (HN) densities (0–100 m) exceeded one order of magnitude (10^1 – 10^3 cells per volume unit). Highest HN and ciliate abundances were found in the surface layer between 5 and 30 m at almost all sites visited during the three sampling seasons (Figure 2). Autumn densities were characterized by low protozoa concentration and secondary subsurface maxima at 40–60 m depth (Figure 2c).

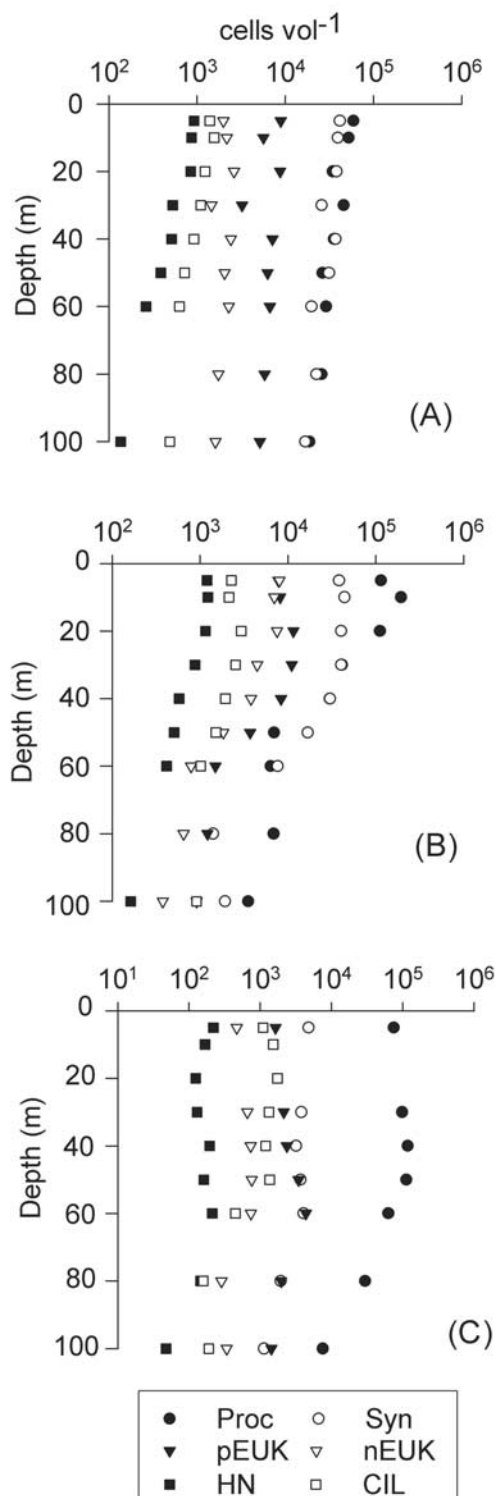


Figure 2. Mean vertical profiles of populations in winter (P1), spring (P2), and autumn (P3). CIL, ciliates; HN, heterotrophic nanoflagellates; Proc, *Prochlorococcus*; Syn, *Synechococcus*; pEUK and nEUK, photosynthetic pico- and nano-eukaryotes, respectively. Units are per liter for ciliates and per milliliter for other microbial groups. Note the logarithmic scale on the x axis.

[16] For heterotrophic nanoflagellates, maximal values ($3760 \text{ cells mL}^{-1}$) occurred at station S3 in spring (P2). The range of depth integrated abundances of HN was similar ($7.7\text{--}10 \times 10^{10} \text{ cells m}^{-2}$) in winter (P1) and autumn (P3, Figure 3a). Slightly lower values were found only at S4 in autumn (P3, $6.5 \times 10^{10} \text{ cells m}^{-2}$). The highest abundance was recorded in spring (P2), when integrated values were over $10^{11} \text{ cell m}^{-2}$ at most of the sampling sites (Figure 3a).

[17] For ciliates, maxima occurred in winter (S3, $1940 \text{ cells L}^{-1}$) and in spring (S2, $1880 \text{ cells L}^{-1}$). Depth integrated values of ciliate abundances varied within the same range ($2.3\text{--}6.5 \times 10^7 \text{ cells m}^{-2}$) during winter (P1) and spring (P2) with the exception of S4 in P2 where densities were unusually high ($12.3 \times 10^7 \text{ cells m}^{-2}$, Figure 3a). In autumn (P3), depth integrated abundance was lower and varied within a narrower range than in winter and spring ($1.2\text{--}2.1 \times 10^7 \text{ cells m}^{-2}$). The ciliate community was dominated by oligotrichs, predominantly *Strombidium* spp., which represented $>70\%$ of the ciliate abundance and biomass during the three sampling periods. The exception was station S4 during P2, where loricate ciliates of *Tintinnus* sp. were dominant contributing over 70% of the ciliate abundance and biomass. A heterogeneous population of loricate ciliates was also dominant in terms of biomass at S4 in autumn (P3). Finally, high tintinnid abundances ($800\text{--}900 \text{ cells mL}^{-1}$) similar to that of naked ciliates were found at the surface of site S3 in winter (P1).

[18] Biomass of HN and ciliates, integrated over the upper 100 m, ranged from 260 to 310, 320 to 1500 and 130 to 155 mg C m^{-2} during winter (P1), spring (P2) and autumn (P3), respectively (Figure 4a). HN biomass exceeded that of ciliates representing $\geq 60\%$ of total protozoa biomass except at stations S2 (54%) and S3 (49%) of the winter cruise (P1) and station S4 (57%) of the spring cruise (P2). For both HN and ciliates, depth integrated biomass and abundance presented similar patterns of seasonal and spatial variations (Figures 3a and 4a).

3.3. Abundance and Biomass of Pico- and Nanophytoplankton

[19] *Prochlorococcus* and *Synechococcus* abundance varied by over an order of magnitude ($10^2\text{--}10^5$ and $10^2\text{--}10^4 \text{ cells mL}^{-1}$ respectively) in the surface layer (0–100 m) during the POMME study. Vertical profiles (0–100 m) of the two photosynthetic prokaryotes were more or less uniform during P1 while surface and subsurface maxima occurred in P2 and P3 respectively (Figure 2). *Synechococcus* reached highest abundances in surface layers during spring (Figure 2b) up to $9.8 \times 10^4 \text{ mL}^{-1}$ at site S1 but were already abundant in winter. Their maximal depth integrated abundances occurred during this season (P1, $3.8 \times 10^{12} \text{ Syn m}^{-2}$). The greatest differences between the two prokaryotic populations occurred in late summer (P3), with increased abundances of *Prochlorococcus* and decreasing abundances of *Synechococcus* down to 100m depth. Integrated abundance of *Prochlorococcus* reached its maximum ($8.8 \times 10^{12} \text{ Proc m}^{-2}$) at that time.

[20] Abundances of photosynthetic picoeukaryotic cells (pEUK) varied by over an order of magnitude ($10^2\text{--}10^5 \text{ cells mL}^{-1}$) during the three cruises while for nano-eukaryotes (nEUK) the range was narrower ($10^2\text{--}10^3 \text{ cells mL}^{-1}$).

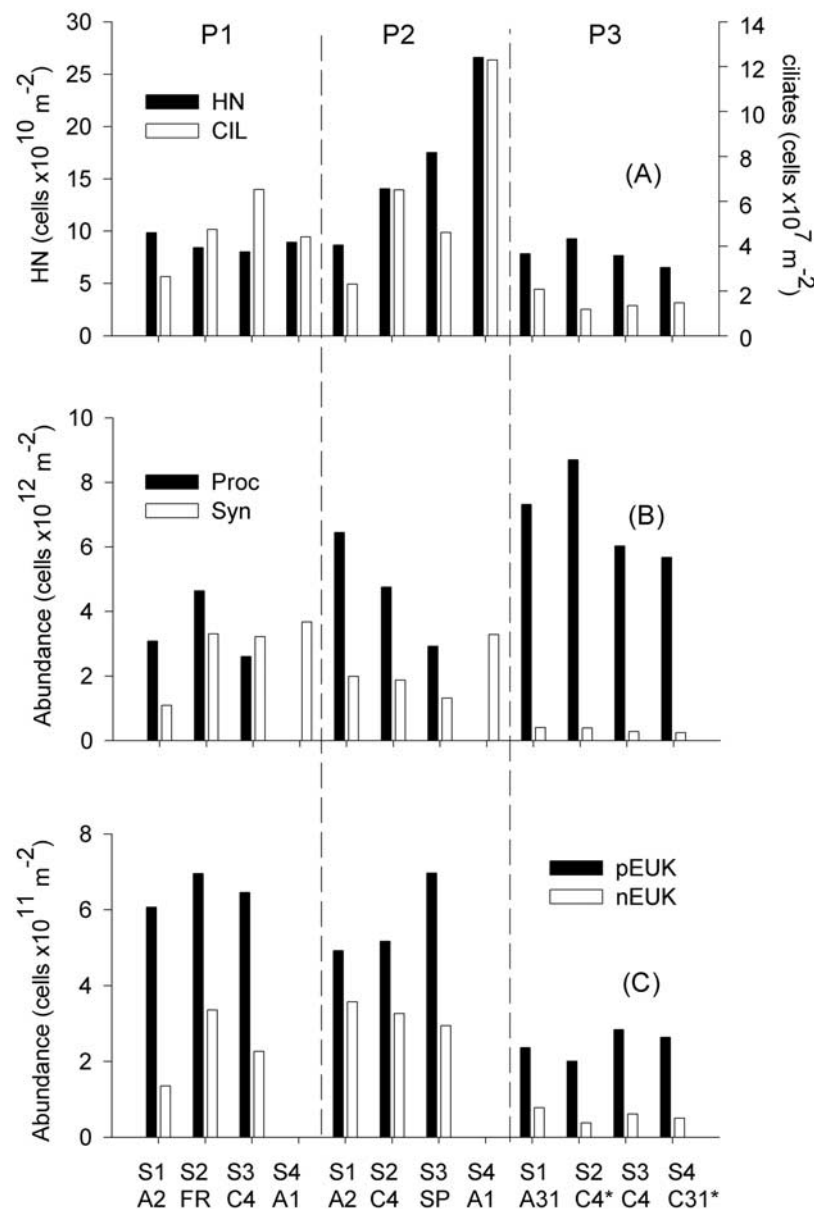


Figure 3. Integrated abundance (0–100 m) of (a) ciliates (CIL) and heterotrophic nanoflagellates (HN), (b) photosynthetic picoprokaryotes (*Prochlorococcus* (Proc) and *Synechococcus* (Syn)), and (c) photosynthetic pico- (pEUK) and nanoeukaryotes (nEUK) at different sampling stations in winter (P1), spring (P2), and autumn (P3). S1, S2, S3, S4, sites; A, anticyclonic eddy; FR, front; C, cyclonic eddy; SP, saddle point (see also Table 1).

As for prokaryotes, maximal abundances occurred in spring ($1.7 \times 10^4 \text{ mL}^{-1}$ and $8.4 \times 10^3 \text{ mL}^{-1}$ for pico- and nanoeukaryotes respectively). Seasonal variation of depth integrated abundance of picoeukaryotes was similar to that of *Synechococcus*. Densities were higher in winter and spring ($>5 \times 10^{11} \text{ cells m}^{-2}$) and decreased significantly in autumn ($<3 \times 10^{11} \text{ cells m}^{-2}$, Figure 3c). Maximal values ($8.3 \times 10^{11} \text{ cells m}^{-2}$) occurred at S2 in winter (P1). The same seasonal pattern of variations was found for PN (Figure 3c).

[21] Autotrophic biomass (pico and nanoplanktonic populations), integrated over the upper 100 m ranged from

1600 to 3350 mg C m^{-2} for different sampling stations during winter (P1) and showed less variation ($2090\text{--}2540 \text{ mg C m}^{-2}$) during spring (P2). The range of values was $690\text{--}890 \text{ mg C m}^{-2}$ during autumn (P3, Figure 4b). *Synechococcus* biomass prevailed over *Prochlorococcus* biomass except in autumn (P3, Figure 4b). The importance of the biomass of picoeukaryotes was intermediate ($130\text{--}470 \text{ mg C m}^{-2}$) between *Prochlorococcus* and *Synechococcus* at most of the sampling sites visited during the three sampling periods. Photosynthetic nanoplankton biomass was approximately equivalent to the sum of the picoautotroph biomasses except in autumn when *Prochlorococcus*

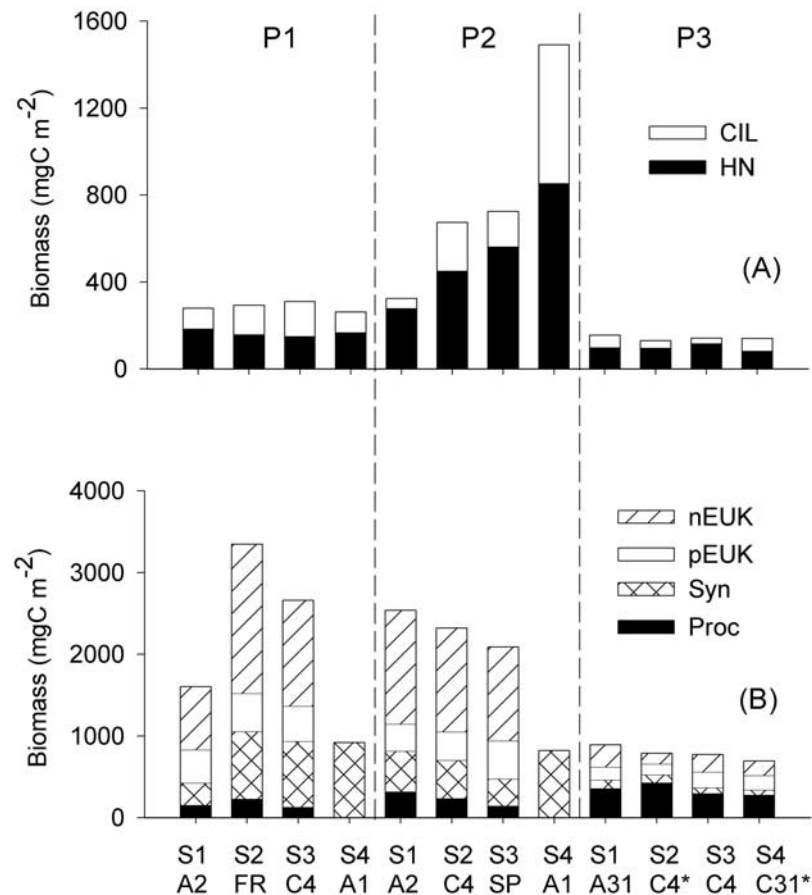


Figure 4. Integrated biomass (0–100 m) of (a) heterotrophs, ciliates (CIL), and heterotrophic nanoflagellates (HN) and (b) autotrophs, *Prochlorococcus* (Proc), *Synechococcus* (Syn), photosynthetic picoeukaryotes (pEUK), and nanoeukaryotes (nEUK) at different sampling stations in winter (P1), spring (P2), and autumn (P3). The x axis is as in Figure 3.

biomass alone accounted for $43 \pm 7\%$ of integrated biomass of phytoplankton belonging to the $<10 \mu\text{m}$ size class.

3.4. Ciliate and Heterotrophic Nanoflagellate Herbivory

[22] Fluorescently labeled prey uptake experiments permit the determination of the feeding characteristics of oligotrichs and tintinnids separately. Concerning ciliates, ingestion rates of pico- plus nanoeukaryotes (pnEUK) varied between 1 and 58 $\text{pnEUK oligo}^{-1} \text{h}^{-1}$ and between 2 and 121 $\text{pnEUK tint}^{-1} \text{h}^{-1}$, for aloricate ciliates and tintinnids respectively (Table 3). Maximal values for aloricate ciliates occurred at S2 (frontal zone) in winter (P1) and for tintinnids at S3 (saddle point), in spring (P2). Both types of predators ingested *Synechococcus* with higher rates than the assemblage of photosynthetic pico- plus nanoeukaryotes (pnEUK) during winter (P1) and spring (P2) and with similar rates during autumn (P3, Table 3). Aloricate ciliate clearance rates on pnEUK as well as on *Synechococcus* were greatest in winter (P1). For tintinnids, maximal values of clearance rates occurred in spring (P2) for both prey types.

[23] Concerning predation by heterotrophic nanoflagellates (HN), ingestion rates of *Synechococcus* and *Prochlorococcus* were significantly lower than those for ciliates (Table 3). *Synechococcus* and *Prochlorococcus* ingestion rates, derived from equations (1) and (2) which relate prey

concentration with flagellate ingestion, were obviously greatest when prey concentration was maximal, in winter (P3) for the former ($0.238 \text{ Syn HN}^{-1} \text{h}^{-1}$) and in spring/autumn for the latter ($0.177 \text{ Proc HN}^{-1} \text{h}^{-1}$, Table 3). Clearance rates on *Synechococcus* were always higher than those on *Prochlorococcus* by a factor which varied between 1.6 and 2.7 except at site S3 in spring (P2) where similar rates were calculated.

[24] Total flux of phytoplankton carbon consumed by the ciliate assemblage was mainly eukaryotic in origin ($>60\%$, Figure 5). Moreover, aloricate ciliates contributed more than tintinnids to the total ciliate herbivory ($82 \pm 18\%$), with the exception of site 4 ($\leq 12\%$) of the spring cruise (P2) where tintinnids became dominant. In comparing carbon, heterotrophic nanoflagellates (HN) ingested *Synechococcus* with significantly higher rates than *Prochlorococcus* during winter (P1) and spring (P2, Figure 5). On the contrary, in autumn (P3), when *Prochlorococcus* was abundant ($8.8 \times 10^{12} \text{ Proc m}^{-2}$, Figure 3b), daily ingestion rates of this prey ($\text{ng C L}^{-1} \text{d}^{-1}$) by HN exceeded ingestion on *Synechococcus* (Figure 5).

3.5. Comparison of Herbivory Fluxes and Primary Production

[25] In order to determine the importance of ciliates and HN in the fate of primary production, ingestion rates in

Table 3. Range of Depth-Averaged Ingestion Rates (IR) and Clearance Rates (CR) Obtained During the Three POMME Cruises (P1, P2, and P3)^a

Predator	Prey Type	IR, prey predator ⁻¹ h ⁻¹			CR, $\mu\text{l predator}^{-1} \text{h}^{-1}$		
		P1	P2	P3	P1	P2	P3
Oligotrichs	pnEUK	8–58	12–32	1–7	1.3–4.3	1.0–2.4	0.6–2.6
Tintinnids	pnEUK	7–54	37–121	2–6	0.8–4.0	3.1–6.7	0.7–3.0
Oligotrichs	Syn	32–67	25–131	2–17	0.5–3.6	0.6–3.1	0.8–2.5
Tintinnids	Syn	17–83	28–517	3–16	0.5–2.2	1.5–11.7	1.4–3.5
HN	Syn	0.033–0.238	0.066–0.155	0.001–0.026	3.5–3.6	3.5–3.6	3.7–6.3
HN	Proc	0.012–0.134	0.012–0.176	0.012–0.177	1.3–1.7	1.3–1.9	1.28–1.3

^aAbbreviations are as follows: HN, heterotrophic nanoflagellates; pnEUK, photosynthetic picoeukaryotes plus nanoplankton; Syn, *Synechococcus*; Proc, *Prochlorococcus*.

carbon units, integrated over the upper 100 m, were compared to primary production integrated to the same layer. Primary production varied between 370 and 806 mg C m⁻² d⁻¹ at sites 1 to 4 during P1. In spring, primary production increased only at the site S1 corresponding to the anticyclonic eddy A2 and remained constant or decreased at the sampling sites located in eddies A1 (S1) and C4 (S2). Maximal values (1174 mg C m⁻² d⁻¹) occurred at site S3 corresponding to a “saddle” point (intermediate zone between four eddies, Table 1). Primary production decreased significantly during P3 and varied between 168 and 242 mg C m⁻² d⁻¹. Size fractionation of primary production showed that photosynthetic cells smaller than 2 μm contributed more than 58% to total primary production except at sites S2 and S4 of spring cruise (P2) where larger cells contributed $\sim 60\%$. The range of ciliate herbivory on pico- and nanoplankton was 25–146, 31–572, and 1–5 mg C m⁻² d⁻¹ for P1, P2, and P3, respectively (Figure 6a). Corresponding values of HN herbivory were 26–82, 74–193, and 2–27 mg C m⁻² d⁻¹. Overall, herbivory of both protozooplankters (ciliates and heterotrophic nanoflagellates) represented 10–57% of the primary production in winter (P1), 13–94% in spring (P2) and 2–14% in autumn (P3, Figure 6a). Protozoan herbivory of small cells (picoeukaryotes and prokaryotes) represented less than

40% of the <2 μm size class primary production during the three sampling periods with the exception of sites S2 (84%) and S4 (120%) of the spring cruise (P2, Figure 6b). The lowest values (<20%) were found during the autumn (P3).

4. Discussion

[26] During our study, maximal abundance and biomass of ciliates and heterotrophic nanoflagellates occurred in spring and were quantitatively similar to the values previously reported for the northeast Atlantic [Burkill *et al.*, 1993; Stoecker *et al.*, 1994]. The taxonomic composition of the ciliate community sampled from the POMME area was dominated by members of the family Strombidiidae (*Strombidium* spp., *L. strobila*, *Tontonia* spp.) as was observed in previous studies [Burkill *et al.*, 1993; Stoecker *et al.*, 1994; Quevedo and Anadón, 2001]. However, in spring (P2), tintinnids reached significantly high abundances locally (maximum 1260 cells L⁻¹), greatly exceeding values usually reported for oceanic provinces [e.g., Stoecker *et al.*, 1994; Leaky *et al.*, 1996; Pitta *et al.*, 2001]. An oceanic bloom of tintinnids has been previously reported for the Cobb Seamount in the eastern subarctic Pacific where abundance reached 1800 cells L⁻¹ [Sime-Ngando *et al.*, 1992]. These authors suggest that physical forcing increases habitat

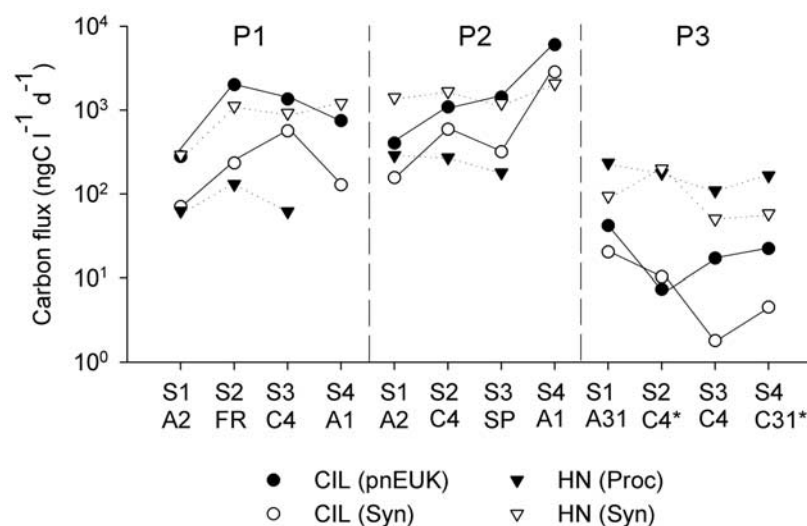


Figure 5. Ingestion rates of photosynthetic pico- plus nanoeukaryotes (pnEUK), *Synechococcus* (Syn), and *Prochlorococcus* (Proc) in carbon units (ng C L⁻¹ d⁻¹) by the assemblage of ciliates (CIL) and/or heterotrophic nanoflagellates (HN). Prey types are in parentheses in the legend. Note the logarithmic scale on the y axis. The x axis is as in Figure 3.

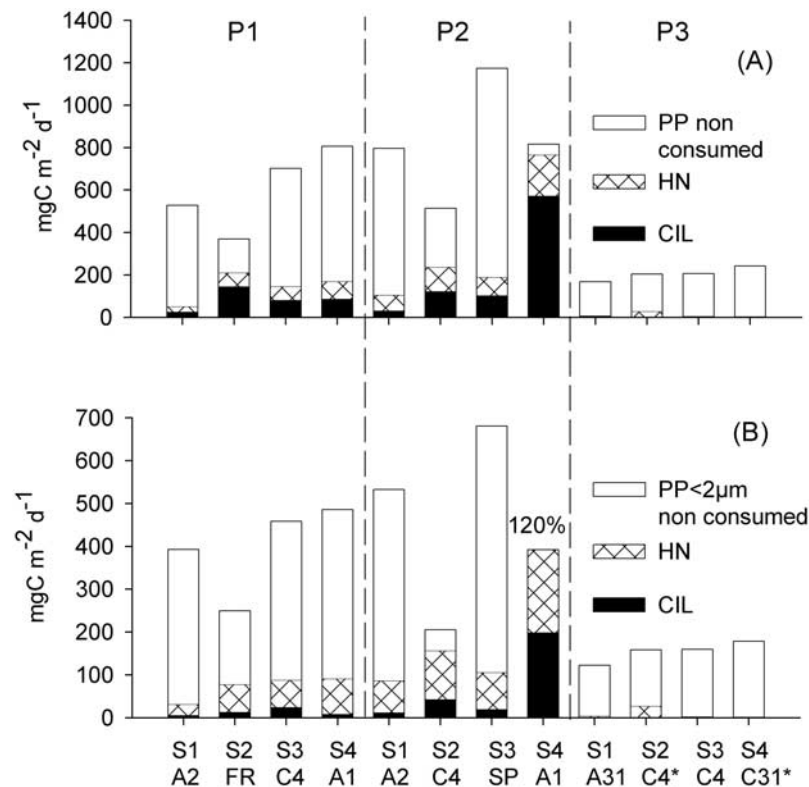


Figure 6. (a) Flux of total primary production plotted with herbivory fluxes of protozoans: CIL, ciliates on nanoeukaryotes, picoeukaryotes, and *Synechococcus*; HN, heterotrophic nanoflagellates on *Prochlorococcus* and *Synechococcus*. (b) Flux of primary production realized by the $<2\text{-}\mu\text{m}$ -sized organisms, plotted with herbivory fluxes of organisms cropping it: CIL, ciliates on picoeukaryotes; HN, heterotrophic nanoflagellates on *Prochlorococcus* and *Synechococcus*. The white bar (primary production (PP) nonconsumed) indicates the remaining part of PP which is not consumed by ciliates or flagellates. The x axis is as in Figure 3.

heterogeneity and scatters biological resources generating microhabitats which favor the growth of opportunistic or physiologically adapted populations. In our study, patches of high *Tintinnus* sp. abundance, at least in the north anticyclone eddy (S4), seemed to be associated with a diatom bloom (*Pseudonitzschia delicatissima*, 20–30 μm [Leblanc *et al.*, 2005]) but the influence of hydrology needs further investigation.

[27] Ingestion rates of photosynthetic eukaryotes by ciliated protozoa have rarely been reported in previous field studies. However, our data ($1\text{--}121 \text{ pnEUK ciliate}^{-1} \text{ h}^{-1}$) were in the range of values reported in laboratory experiments [e.g., Verity, 1988; Bernard and Rassoulzadegan, 1990] although these studies cannot accurately simulate natural conditions. In autumn (P3), ingestion rates ($1\text{--}7 \text{ pnEUK ciliate}^{-1} \text{ h}^{-1}$) were similar to values reported for the oligotrophic Takapoto Atoll ($2.4 \pm 0.8 \text{ algae ciliate}^{-1} \text{ h}^{-1}$) by Sakka *et al.* [2000]. Moreover, many laboratory [Verity, 1988; Caron *et al.*, 1991; Dolan and Šimek, 1997; Christaki *et al.*, 1998, 1999] as well as field studies [Sherr *et al.*, 1991; Bernard and Rassoulzadegan, 1993; Šimek *et al.*, 1995] have shown that ciliates are potential predators of cyanobacteria even if their nutritional value is uncertain [Verity, 1988; Christaki *et al.*, 1999]. Ingestion rates of these studies ($0\text{--}395 \text{ Syn ciliate}^{-1} \text{ h}^{-1}$), when reported [Verity, 1988; Bernard and Rassoulzadegan, 1993; Šimek *et al.*,

1995; Christaki *et al.*, 1999], overlap with the range we found during POMME ($2\text{--}300 \text{ Syn ciliate}^{-1} \text{ h}^{-1}$). Higher rates were measured exclusively for loricate ciliates ($517 \text{ Syn tintinnid}^{-1} \text{ h}^{-1}$) at the surface of the north anticyclonic eddy (S4) in spring (P2). Overall, ingestion of phytoplankton cells by both aloricate ciliates and tintinnids presented a statistically significant strong relationship with prey concentration (Spearman's $r \geq 0.7$, $p < 0.0001$, $n \geq 20$, for both pnEUK and *Synechococcus*) explaining increased grazing during the development of the phytoplankton, in winter (P1) and spring (P2).

[28] It is noteworthy that in spring (P2) large aloricate ciliates ($>30 \mu\text{m}$), which ingest nanophytoplankton more efficiently than smaller ones [Rassoulzadegan *et al.*, 1988], increased in relative abundance within the ciliate assemblage (results not shown). Similarly, during the same period, nanophytoplankton also increased in relative abundance within the photosynthetic eukaryotic assemblage. However, aloricate ciliate clearance rates on the sum of pico- and nanoeukaryotes did not increase as expected. This suggests a competition with tintinnids which developed in spring and presented higher clearance rates on the assemblage of photosynthetic eukaryotes than aloricate taxa (Table 3).

[29] The results obtained using equations (1) and (2) [Christaki *et al.*, 2002] showed that heterotrophic nanoflagellate ingestion rates of *Synechococcus* ($0.001\text{--}0.238$

Table 4. Microzooplankton Herbivory in the Northeast Atlantic Ocean

Location	Season	Method	%PP ^a	Source
60°N, 20°W	midsummer	dilution	39	<i>Burkill et al.</i> [1993]
56°N, 20°W	midsummer	dilution	80	
52°N, 20°W	midsummer	dilution	115	
47°N, 20°W	midsummer	dilution	101	
46°20'N, 17°50'W	spring middle to late bloom	dilution	37–100	<i>Verity et al.</i> [1993] <i>Gifford et al.</i> [1995]
59°N, 21°W	spring bloom	dilution	0	
59°N, 21°W	spring postbloom	dilution	100	
59°N, 21°W	summer	dilution	41	<i>Stelfox-Widdicombe et al.</i> [2000]
60°N, 20°W	summer	dilution	65–167	
37°N, 20°W	summer	dilution	35–228	
28°–36°N, 22°–32°W	summer–spring	dilution	79–109	<i>Quevedo and Anadón</i> [2001] this study this study this study
39°–45°N, 16°–22°W	winter	FLP ^b	10–57 (8–31)	
39°–45°N, 16°–22°W	spring	FLP ^b	13–94 (16–120)	
39°–45°N, 16°–22°W	autumn	FLP ^b	2–14 (1–17)	

^aPercentage of primary production (PP) consumed. In parentheses is the grazing impact on PP due to cells smaller than 2 μm .

^bFluorescent labeled prey.

Syn HN⁻¹ h⁻¹) were in the range (0.0008–2.6 Syn HN⁻¹ h⁻¹) reported in studies conducted in offshore [Kuosa, 1991; Christaki et al., 2001] or coastal waters [Caron et al., 1991; Dolan and Šimek, 1999]. Grazing on *Prochlorococcus* is usually measured by indirect methods based on the disappearance of prey in the experimental bottles [Kuipers and Witte, 2000]. Christaki et al. [2001] estimated ingestion rates which varied from 0.001 to 0.31 Proc HN⁻¹ h⁻¹ in the oligotrophic Mediterranean Sea. In our study, ingestion on *Prochlorococcus* varied in a narrower range (0.012–0.177 Proc HN⁻¹ h⁻¹) and presented an inverted pattern of seasonal variations compared to *Synechococcus* ingestion, reflecting the contrasting seasonal evolution of the abundance of the two prokaryotes.

[30] Although ciliate grazing on *Synechococcus* was found to be more than two orders of magnitude higher than that of nanoflagellates, total ciliate consumption was lower than that of HN because of their relatively lower abundance (Figure 5). Moreover, as the per cell carbon content of photosynthetic eukaryotes (1–5.6 pg cell⁻¹) was higher than that of *Synechococcus* (250 fg cell⁻¹), carbon flux through the consumption of the photosynthetic eukaryotes by the ciliate assemblage exceeded that attributed to the consumption of *Synechococcus* (Figure 5).

[31] To compare different aquatic systems in their efficiency to recycle primary production through predator consumption, carbon flux is usually expressed as the percentage of primary production ingested by predators. In our study, this percentage varied from 2 to 94% between different sampling sites and seasons. Ciliate consumption represented 1–75% of total primary production exceeding or being similar to that of HN (1–24%, Figure 6a) at most of the sampling sites. In previous studies, primary production consumption by ciliates in different environments varied between 7 and >60% [Beers and Stewart, 1967; Burkill, 1982; Rassoulzadegan and Etienne, 1981; Leppanen and Bruun, 1986; Dolan and Marassé, 1995; Dolan et al., 1999; Pérez et al., 2000]. Size fractionation of primary production showed that HN had a greater impact than ciliates on the <2 μm fraction, contributing more than 70% of total consumption in this size fraction except at the north anticyclonic eddy (S4) in spring (P2) where the contribution of the two protozoan groups was similar.

[32] The wide range of the percentage of primary production consumed (2–94%) indicates that the coupling

between primary production (PP) and predators presented spatial and temporal variations reflecting the evolution of the bloom and differences in the structure of the phytoplankton community. Heterotrophic nanoflagellates and ciliates seemed to control phytoplankton at least in the frontal zone (S2) in winter (57% of PP) as well as at the cyclonic eddy C4 (S2, 46%) and the north anticyclonic eddy A1 (S4, 94%) in spring. Tintinnid impact was particularly important (69% of the PP), greatly exceeding the values previously reported (<1–38% [Kopylov and Tumantseva, 1987; Heinbokel and Beers, 1979]), in the site located in the anticyclonic eddy A1 (S4) in spring (P2). Overall, these results are in the range of values (35 to >100%) that have been reported in other studies conducted in adjacent provinces of the northeast Atlantic, using community approaches (Table 4).

[33] Consumption by protozoa at the anticyclonic eddy A2 in the south was lower than 15% of the primary production during winter (P1) and spring (P2) experiments (Figures 6a and 6b). A possible explanation is that as the spring bloom in the study area was initiated in the southwest [Fernandez et al., 2005], at this eddy we likely sampled before-bloom (P1) and after-bloom (P2) conditions.

[34] Although *Prochlorococcus* became dominant during autumn (Figures 3b and 4b), the protozoan assemblage (HN and ciliates) had a much lower impact on primary production ($\leq 14\%$), despite the fact that heterotrophic nanoflagellates are generally considered to be the major predators of small-sized prey [Rassoulzadegan et al., 1988; Caron et al., 1991; Kuipers and Witte, 2000]. The observations of low grazing during this period is in agreement with the results of Stelfox-Widdicombe et al. [2000] who found that microzooplankton was not effective in influencing the production of prochlorophytes in the subtropical northeast Atlantic. Some appendicularians have been quantified in high amounts in autumn at some sites which could have also an impact on the fate of small primary producers [Gorsky et al., 1999].

[35] Overall, this study has illustrated differences in ciliate and heterotrophic nanoflagellate herbivorous impact on small size phytoplankton, associated with different hydrological structures and sampling seasons in the northeast Atlantic. Our findings suggest that the amount of primary production channeled into the microbial food web through protozoa consumption depends on the composition

of the phytoplankton community and on the stage of development of phytoplankton bloom. During winter and spring, high *Synechococcus* and photosynthetic eukaryotic abundance and biomass resulted in higher protozoan biomass and in a relatively strong coupling between predators and prey. Conversely, when *Prochlorococcus* became dominant during the autumn, a smaller percentage of primary production was consumed by ciliates and heterotrophic nanoflagellates.

[36] Results of the partial pressure of CO₂ (pCO₂ (L. Merlivat, unpublished data, 2004)) measured by drifting buoys during POMME showed that the study area is a CO₂ sink during winter and spring and a CO₂ source during autumn. Our findings indicated that heterotrophic nanoflagellates and ciliates were relatively more important in determining the fate of phyto-genic carbon in spring. To what extent CO₂ absorption in spring is related to protozoan grazing activity? *Burkill et al.* [1993] formulated the hypothesis that although microzooplanktonic grazing is supposed to hold back some fraction of the carbon from the "biological pump," it could equally be argued that this pathway is implicitly efficient in exporting phytoplankton from the surface layers into deep water via a two or more grazing steps. Although our data seem to corroborate this hypothesis, we are still far from confirming it, since we have no information on the fate of protozoan biomass and thus we do not know how much of it turns up in faecal pellets. It should be also noted that variations in community structure of both prey and predators are crucial in this process. Therefore the study of pico- and nanoplankton diversity and grazing behavior are essential in the understanding of carbon flow within aquatic ecosystems and consequently in ameliorating our capability to predict the future course of atmospheric CO₂.

[37] **Acknowledgments.** This work is a contribution to the POMME program. Financial support was provided by the CNRS-INSU, France. We would like to thank A. Dalby for improving the manuscript with his suggestions; his support is greatly appreciated. Special thanks to S. Papaspyrou for his contribution to the designing of the figures and to A. Maixandau and M. Thyssen for their help with flow cytometry sample analysis. We gratefully acknowledge two anonymous reviewers for their suggestions to improve the manuscript.

References

- Beers, J. R., and G. L. Stewart (1967), Microzooplankton in the euphotic zone at five locations across the California Current, *J. Fish. Res. Board Can.*, **24**, 2053–2068.
- Bernard, C., and F. Rassoulzadegan (1990), Bacteria or microflagellates as a major food source for marine ciliates: Possible implications for the microzooplankton, *Mar. Ecol. Prog. Ser.*, **64**, 147–155.
- Bernard, C., and F. Rassoulzadegan (1993), The role of picoplankton (cyanobacteria and plastidic picoflagellates) in the diet of tintinnids, *J. Plankton Res.*, **15**, 361–373.
- Børsheim, K. Y., and G. Bratbak (1987), Cell volume to cell carbon conversion factors for a bacterivorous *Monas* sp. enriched from sea water, *Mar. Ecol. Prog. Ser.*, **36**, 171–179.
- Burkill, P. H. (1982), Ciliates and other microplankton components of nearshore food-web: Standing stocks and production processes, *Ann. Inst. Oceanogr. Paris*, **58**, 335–350.
- Burkill, P. H., E. S. Edwards, A. W. G. John, and M. A. Sleight (1993), Microzooplankton and their herbivorous activity in the northeastern Atlantic Ocean, *Deep Sea Res., Part II*, **40**, 479–493.
- Burkill, P. H., E. S. Edwards, and M. A. Sleight (1995), Microzooplankton and their role in controlling phytoplankton growth in the marginal ice zone of the Bellingshausen Sea, *Deep Sea Res., Part II*, **42**, 1227–1290.
- Cailliau, C., H. Claustre, F. Vidussi, D. Marie, and D. Vaultot (1996), Carbon biomass, and gross growth rates as estimated from 14C pigment labelling, during photoacclimation in *Prochlorococcus* CCMP 1378, *Mar. Ecol. Prog. Ser.*, **145**, 209–221.
- Caron, D. A., E. L. Lim, G. Miceli, J. B. Waterbury, and F. W. Valois (1991), Grazing and utilization of chroococcoid cyanobacteria and heterotrophic bacteria by protozoa in laboratory cultures and a coastal plankton community, *Mar. Ecol. Prog. Ser.*, **76**, 205–217.
- Christaki, U., J. R. Dolan, S. Pelegri, and F. Rassoulzadegan (1998), Consumption of picoplankton-size particles by marine ciliates: Effects of physiological state of the ciliate and particle quality, *Limnol. Oceanogr.*, **43**, 458–464.
- Christaki, U., S. Jacquet, J. R. Dolan, D. Vaultot, and F. Rassoulzadegan (1999), Growth and grazing on *Prochlorococcus* and *Synechococcus* by two marine ciliates, *Limnol. Oceanogr.*, **44**, 52–61.
- Christaki, U., A. Giannakourou, F. Van Wambeke, and G. Grégori (2001), Nanoflagellate predation on auto- and heterotrophic picoplankton in the oligotrophic Mediterranean Sea, *J. Plankton Res.*, **23**, 1297–1310.
- Christaki, U., C. Courties, H. Karayanni, A. Giannakourou, C. Maravelias, A. K. Kormas, and P. Lebaron (2002), Dynamic characteristics of *Prochlorococcus* and *Synechococcus* consumption by bacterivorous nanoflagellates, *Microbial Ecol.*, **43**, 341–352.
- Dolan, J. R., and C. Marassé (1995), Planktonic ciliate distribution relative to a deep chlorophyll maximum: Catalan Sea, N. W. Mediterranean, June 1993, *Deep Sea Res., Part I*, **42**, 1965–1987.
- Dolan, J. R., and K. Šimek (1997), Processing of ingested matter in *Strombidium sulcatum*, a marine ciliate (Oligotrichida), *Limnol. Oceanogr.*, **42**, 393–397.
- Dolan, J. R., and K. Šimek (1999), Diel periodicity in *Synechococcus* populations and grazing by heterotrophic nanoflagellates: Analysis of food vacuole contents, *Limnol. Oceanogr.*, **44**, 1565–1570.
- Dolan, J. R., F. Vidussi, and H. Claustre (1999), Planktonic ciliates in the Mediterranean Sea: Longitudinal trends, *Deep Sea Res., Part I*, **46**, 2025–2039.
- Fernandez, I. C., P. Raimbault, G. Caniaux, N. Garcia, and P. Rimmelin (2005), Influence of mesoscale eddies on nitrate distribution during the POMME program in the northeast Atlantic Ocean, *J. Mar. Syst.*, **55**, 155–175.
- Fortier, L., J. Le Fevre, and L. Legendre (1994), Export of biogenic carbon to fish and deep ocean: The role of large planktonic micropredators, *J. Plankton Res.*, **16**, 809–839.
- Gifford, D. J., L. M. Fessenden, P. R. Garrahan, and E. Martin (1995), Grazing by microzooplankton and mesozooplankton in the high-latitude North Atlantic Ocean: Spring versus summer dynamics, *J. Geophys. Res.*, **100**, 6665–6675.
- Gilron, G. L., and D. H. Lynn (1989), Assuming a 50% cell occupancy of the lorica overestimates tintinnid ciliate biomass, *Mar. Biol.*, **103**, 413–416.
- Gorsky, G., M. J. Chrétiennot-Dinet, J. Blanchot, and I. Palazzoli (1999), Picoplankton and nanoplankton aggregation by appendicularians: Faecal pellet contents of *Meglocercus huxleyi* in the equatorial Pacific, *J. Geophys. Res.*, **104**, 3381–3390.
- Heinbokel, J. F., and J. R. Beers (1979), Studies on the functional role of tintinnids in the Southern California Bight. III. Grazing impact of natural assemblages, *Mar. Biol.*, **52**, 23–32.
- Jørgensen, E. (1924), Mediterranean Tintinnidae, in *Report on the Danish Oceanographical Expeditions 1908–1910 to the Mediterranean and Adjacent Seas*, vol. 2, J.3, edited by A. F. Høst et al., 110 pp., Copenhagen.
- Kana, T., and P. M. Glibert (1987), Effect of irradiances up to 2000 $\mu\text{E m}^{-2} \text{s}^{-1}$ on marine *Synechococcus* WH 7803-I: Growth pigmentation and cell composition, *Deep Sea Res., Part A*, **34**, 479–516.
- Karayanni, H., U. Christaki, F. Van Wambeke, and A. P. Dalby (2004), Evaluation of double formalin–Lugol's fixation in assessing number and biomass of ciliates: An example of estimations at mesoscale in NE Atlantic, *J. Microbiol. Methods*, **56**, 349–358.
- Kofoid, C. A., and A. S. Campbell (1929), A conspectus of the marine and fresh-water Ciliata belonging to the suborder Tintinninea, with descriptions of new species principally from the Agassiz Expedition to the Eastern Tropical Pacific, 1904–1905, in *University of California Publications in Zoology*, vol. 34, 403 pp., Univ. of Calif. Press, Berkeley.
- Kopylov, A. I., and N. I. Tumantseva (1987), Analysis of the contents of tintinnid vacuoles and evaluation of their contribution to the consumption of phytoplankton off the Peru coast, *Oceanology*, **27**, 243–247.
- Kuipers, B. R., and H. J. Witte (2000), *Prochlorophytes* as secondary prey for heterotrophic nanoflagellates in the deep chlorophyll maximum layer of the (sub)tropical North Atlantic, *Mar. Ecol. Prog. Ser.*, **204**, 53–63.
- Kuosa, H. (1991), Picoplanktonic algae in the northern Baltic Sea: Seasonal dynamics and flagellate grazing, *Mar. Ecol. Prog. Ser.*, **73**, 269–271.
- Landry, M. R., and R. P. Hassett (1982), Estimating the grazing impact of marine microzooplankton, *Mar. Biol.*, **67**, 283–288.

- Leaky, R. J. G., P. H. Burkill, and M. A. Sleight (1996), Planktonic ciliates in the northwestern Indian Ocean: Their abundance and biomass in waters of contrasting productivity, *J. Plankton Res.*, 18, 1063–1071.
- Leblanc, K., A. Leynaert, I. C. Fernandez, P. Rimmelin, T. Moutin, P. Raimbault, J. Ras, and B. Queguiner (2005), A seasonal study of diatom dynamics in the North Atlantic during the POMME experiment (2001): Evidence for Si limitation of the spring bloom, *J. Geophys. Res.*, doi:10.1029/2004JC002621, in press.
- Leppanen, J. M., and J. E. Bruun (1986), The role of pelagic ciliates including the autotrophic *Mesodinium rubrum* during the spring bloom of 1982 in the open northern Baltic proper, *Ophelia*, 4, 147–157.
- Lewis, M. R. (1989), The variegated ocean: View from space, *New Sci.*, 1685, 37–40.
- Maar, M., T. G. Nielsen, K. Richardson, U. Christaki, O. S. Hansen, T. Zervoudaki, and E. D. Christou (2002), Spatial and temporal variability of food web structure during the spring bloom in the Skagerrak, *Mar. Ecol. Prog. Ser.*, 239, 11–29.
- Maeda, M. (1986), An illustrated guide to the species of the families Halteridiidae and Strobiliidiidae (Oligotrichida, Ciliophora) free swimming protozoa common in the aquatic environment, in *Bulletin of the Ocean Research Institute University of Tokyo*, vol. 21, edited by T. Asai et al., 67 pp., University of Tokyo.
- Maeda, M., and P. G. Carey (1985), An illustrated guide to the species of the family Strombidiidae (Oligotrichida, Ciliophora), free swimming protozoa common in the aquatic environment, in *Bulletin of the Ocean Research Institute University of Tokyo*, vol. 19, edited by T. Asai et al., 68 pp., University of Tokyo.
- Maixandeau, A., et al. (2005), Microbial community production, respiration, and structure of the microbial food web of an ecosystem in the northeastern Atlantic Ocean, *J. Geophys. Res.*, doi:10.1029/2004JC002694, in press.
- Montagnes, D. J. S., and D. H. Lynn (1991), Taxonomy of Choreotrichs, the major marine planktonic ciliates, with emphasis on the aloricate forms, *Mar. Microbiol. Food Webs*, 5, 59–74.
- Moutin, T., and P. Raimbault (2002), Primary production, carbon export and nutrients availability in western and eastern Mediterranean Sea in early summer 1996, *J. Mar. Syst.*, 33–34, 273–288.
- Pace, M. L., G. B. McManus, and S. E. G. Findlay (1990), Planktonic community structure determines the fate of bacterial production in a temperate lake, *Limnol. Oceanogr.*, 35, 795–808.
- Paillet, J., and M. Arhan (1996), Shallow pycnoclines and mode water subduction in the eastern North Atlantic, *J. Phys. Oceanogr.*, 26, 96–114.
- Pérez, M. T., J. R. Dolan, F. Vidussi, and E. Fukai (2000), Diel vertical distribution of planktonic ciliates within the surface layer of the NW Mediterranean (May 1995), *Deep Sea Res., Part I*, 47, 479–503.
- Pitta, P., A. Giannakourou, and U. Christaki (2001), Planktonic ciliates in the oligotrophic Mediterranean Sea: Longitudinal trends of standing stocks, distributions and analysis of food vacuole contents, *Aquat. Microbiol. Ecol.*, 24, 297–311.
- Porter, K. G., and Y. S. Feig (1980), The use of DAPI for identifying and counting aquatic microflora, *Limnol. Oceanogr.*, 25, 943–948.
- Putt, M., and D. K. Stoecker (1989), An experimentally determined carbon: Volume ratio for marine “oligotrichous” ciliates from estuarine and coastal waters, *Limnol. Oceanogr.*, 34, 1097–1103.
- Quevedo, M., and R. Anadón (2001), Protist control of phytoplankton growth in the subtropical north-east Atlantic, *Mar. Ecol. Prog. Ser.*, 221, 29–38.
- Rassoulzadegan, F., and M. Etienne (1981), Grazing of the tintinnid *Stenosmella ventricosa* (Clap. & Lachm.) Jörg. on the spectrum of naturally occurring particulate matter from a Mediterranean neritic area, *Limnol. Oceanogr.*, 26, 258–270.
- Rassoulzadegan, F., M. Laval-Peuto, and R. W. Sheldon (1988), Partitioning of the food ration of marine ciliates between pico- and nanoplankton, *Hydrobiologia*, 159, 75–88.
- Rublee, P. A., and C. L. Gallegos (1989), Use of fluorescently labelled algae (FLA) to estimate microzooplankton grazing, *Mar. Ecol. Prog. Ser.*, 51, 221–227.
- Sakka, A., L. Legendre, M. Gosselin, and B. Delesalle (2000), Structure of the oligotrophic planktonic food web under low grazing of heterotrophic bacteria: Takapoto Atoll, French Polynesia, *Mar. Ecol. Prog. Ser.*, 197, 1–17.
- Sanders, R. W., U. G. Berninger, E. L. Lim, P. F. Kemp, and D. A. Caron (2000), Heterotrophic and mixotrophic nonplankton predation on picoplankton in the Sargasso Sea and Georges Bank, *Mar. Ecol. Prog. Ser.*, 192, 103–118.
- Sherr, B. F., E. B. Sherr, and R. D. Fallon (1987), Use of monodispersed, fluorescently labeled bacteria to estimate in situ protozoan bacterivory, *Appl. Environ. Microbiol.*, 53, 958–965.
- Sherr, E. B., B. F. Sherr, and J. McDaniel (1991), Clearance rates of <6 µm fluorescently labelled algae (FLA) by estuarine protozoa: Potential grazing impact of flagellates and ciliates, *Mar. Ecol. Prog. Ser.*, 69, 81–92.
- Šimek, K., J. Bobková, M. Macek, J. Nedoma, and R. Psenner (1995), Ciliate grazing on picoplankton in a eutrophic reservoir during the summer phytoplankton maximum: A study at the species community level, *Limnol. Oceanogr.*, 40, 1077–1090.
- Sime-Ngando, T., K. Juniper, and A. Vézina (1992), Ciliated protozoan communities over Cobb Seamount: Increase in biomass and spatial patchiness, *Mar. Ecol. Prog. Ser.*, 89, 37–51.
- Stelfox-Widdicombe, C. E., E. S. Edwards, P. H. Burkill, and M. A. Sleight (2000), Microzooplankton grazing activity in the temperate and sub-tropical NE Atlantic: Summer 1996, *Mar. Ecol. Prog. Ser.*, 208, 1–12.
- Stoecker, D. K., M. E. Sieracki, P. G. Verity, A. E. Michaels, E. Haugen, P. H. Burkill, and E. S. Edwards (1994), Nanoplankton and protozoan microzooplankton during the JGOFS North Atlantic Bloom Experiment: 1989 and 1990, *J. Mar. Biol. Assoc.*, 74, 427–443.
- Troussellier, M., C. Courties, and S. Zettlemayer (1995), Flow cytometric analysis of coastal lagoon bacterioplankton and picophytoplankton: Fixation and storage effects, *East. Coastal Shelf Res.*, 40, 621–623.
- Tsuda, A., K. Furuya, and T. Nemoto (1989), Feeding of micro- and macrozooplankton at the subsurface chlorophyll maximum in the subtropical North Pacific, *J. Explor. Mar. Biol. Ecol.*, 132, 41–52.
- Verity, P. G. (1988), Chemosensory behavior in marine planktonic ciliates, *Bull. Mar. Sci.*, 43, 772–782.
- Verity, P. G., D. K. Stoecker, M. E. Sieracki, and J. R. Nelson (1993), Grazing, growth and mortality of microzooplankton during the 1989 North Atlantic spring bloom at 47°N, 18°W, *Deep Sea Res., Part I*, 40, 1793–1814.
- Weeks, A., et al. (1993), The physical and chemical environment and changes in community structure associated with bloom evolution: The Joint Global Flux Study North Atlantic Bloom Experiment, *Deep Sea Res., Part II*, 40, 347–368.

U. Christaki, Université du Littoral Côte d'Opale, UMR CNRS-INSU 8013, MREN, 32 avenue Foch, F-62930 Wimereux, France. (urania.christaki@mren2.univ-littoral.fr)

M. Denis, H. Karayanni, and F. Van Wambeke, Laboratoire de Microbiologie, Géochimie et Ecologie Marines, CNRS/INSU, UMR 6117, Case 901, Centre d'Océanologie de Marseille, Université de la Méditerranée, Campus de Luminy, F-13288 Marseille Cedex 9, France. (denis@com.univ-mrs.fr; hera@com.univ-mrs.fr; wambeke@com.univ-mrs.fr)

T. Moutin, Laboratoire d'Océanographie et de Biogéochimie, CNRS/INSU, UMR 6535, Case 901, Centre d'Océanologie de Marseille, Université de la Méditerranée, Campus de Luminy, F-13288 Marseille Cedex 9, France. (thierry.moutin@com.univ-mrs.fr)